

**NANO EXPRESS**

**Open Access**

# Biosynthesis of gold nanoparticles assisted by the intracellular protein extract of *Pycnopus sanguineus* and its catalysis in degradation of 4-nitroaniline

Chaohong Shi<sup>1</sup>, Nengwu Zhu<sup>1,2\*</sup>, Yanlan Cao<sup>1</sup> and Pingxiao Wu<sup>1,2</sup>

## Abstract

The development of green procedure for the synthesis of gold nanoparticles (AuNPs) has gained great interest in the field of nanotechnology. Biological synthetic routes are considered to be environmentally benign and cost-effective. In the present study, the feasibility of AuNPs' synthesis via intracellular protein extract (IPE) of *Pycnopus sanguineus* was explored. The characteristics of generated particles of formation, crystalline nature, and morphology and dimension were analyzed by UV-vis spectroscopy, X-ray diffraction (XRD) and transmission electron microscopy (TEM), respectively. UV-vis spectra exhibited strong absorption peaks in 520 to 560 nm, indicating the formation of AuNPs. XRD analysis revealed that the formed AuNPs were purely crystalline in nature. TEM observation showed that AuNPs with various shapes including spherical, pseudo-spherical, triangular, truncated triangular, pentagonal, and hexagonal, ranging from several to several hundred nanometers, were synthesized under different conditions. The average size of AuNPs decreased from 61.47 to 29.30 nm as the IPE addition increased from 10 to 80 mL. When the initial gold ion concentration changed from 0.5 to 2.0 mM, the average size rose from 25.88 to 51.99 nm. As in the case of solution pH, the average size was 84.29 nm with solution pH of 2.0, which diminished to 6.07 nm with solution pH of 12.0. Fourier transform infrared (FTIR) analysis implied that the functional groups including hydroxyl, amine, and carboxyl were involved in the reduction of gold ions and stabilization of AuNPs. The catalysis results showed that 0.019 mg of AuNPs with average size of 6.07 nm could catalyze the complete degradation of 12.5  $\mu$ mol of 4-nitroaniline within 6 min and the degradation rate increased drastically with the addition of AuNPs. All the results suggested that the IPE of *P. sanguineus* could be potentially applied for the eco-friendly synthesis of AuNPs.

**Keywords:** Gold nanoparticles; Intracellular protein extract; *Pycnopus sanguineus*; Biosynthesis; Catalysis

## Background

Nanotechnology is becoming the focus of scientific researches all over the world during the last few decades. The synthesis of noble metal nanoparticles with controlled morphology and dimension exhibits outstanding importance in this field, as metal particles at nanoscale possess many properties significantly different from those of the corresponding bulk materials [1]. Particularly, gold

nanoparticles (AuNPs) are of the most importance owing to their wide applications in optics, electronics, catalysis, and biomedicine [2,3].

Various physical and chemical approaches are available to synthesize AuNPs [1], while almost all those methods are energy or capital intensive. What is more, many toxic chemicals including sodium borohydride ( $\text{NaBH}_4$ ), surfactants, or thiol groups are involved, thus precluding the applications of the produced AuNPs in many clinical and biological areas. Therefore, the development of a clean, cost-effective, and environmentally benign process to synthesize AuNPs is in urgent demand.

\* Correspondence: nwzhu@scut.edu.cn

<sup>1</sup>School of Environment and Energy, South China University of Technology, Guangzhou 510006, China

<sup>2</sup>The Key Laboratory of Pollution Control and Ecosystem Restoration in Industry Clusters of Ministry of Education, Guangzhou 510006, China

Currently, a lot of biological materials such as bacteria, fungi, algae, and plants have been reported to synthesize AuNPs [4-7]. Most researches focused on biosynthesis of AuNPs with the whole cells, and the AuNPs were deposited on the cell wall or in the cytoplasmic region [4,8]. Cell-free spent medium or cell-free extract, containing the functional substances including secreted metabolites or eluted extracellular polymeric substances, were also applied to synthesize AuNPs [9,10]. As we know, fungi are able to secrete more proteins, produce more biomass, and show higher metal tolerance and bioaccumulation ability [11]. So far, many fungal species such as *Rhizopus oryzae* [11], *Neurospora crassa* [12], *Trichoderma harzianum* [13], *Aspergillus oryzae* [9], *Helminthosporium solani* [14], *Fusarium semitectum* [15], and *Candida albicans* [16] have been reported to successfully synthesize AuNPs either through extra- or intracellular manners. Thus, fungi are considered to be the most promising candidates for AuNPs synthesis.

The catalytic property of AuNPs is widely concerned from the standpoint of application, especially in the case of degrading contaminants in wastewater. Previous reports have revealed that AuNPs synthesized in biological systems could effectively catalyze the degradation of 4-nitrophenol [2,17]. The biosynthesized AuNPs showed much better catalytic activity than chemically synthesized AuNPs [11]. In addition, biosynthesized AuNPs could even be reused for many rounds [18].

In the present study, for the first time, we used the intracellular protein extracts (IPE) of a white rot fungal strain *Pycnoporus sanguineus* (*P. sanguineus*) to synthesize AuNPs. It was reported that *P. sanguineus* could produce large amount of reductase such as laccases, which might enable us to synthesize AuNPs by the fungus [19,20]. The effects of reaction parameters including IPE addition, initial gold ion concentration, and solution pH on the characteristics of synthesized AuNPs were evaluated. The catalytic activity of biosynthesized AuNPs was investigated in degradation of 4-nitroaniline (4-NA).

## Methods

### Materials

The reagents used were of analytical grade. Chloroauric acid ( $\text{HAuCl}_4 \cdot 3\text{H}_2\text{O}$ ), 4-NA,  $\text{NaBH}_4$ , dextrose,  $\text{KH}_2\text{PO}_4$ ,  $\text{MgSO}_4 \cdot 7\text{H}_2\text{O}$  and other chemicals were purchased from Aladdin, Shanghai, China. Chloroauric acid was dissolved in ultrapure water to prepare stock solution for further use.

### Fungal strain, growth conditions, and preparation of IPE

The fungal strain *P. sanguineus* (CGMCC 5.00815) was purchased from China General Microbiological Culture Collection Center, maintained on comprehensive potato

dextrose agar (PDA) slants, and kept in refrigerator for further use. To obtain biomass for AuNPs synthesis, *P. sanguineus* was inoculated into nutrition liquid medium, followed by incubation on a rotary shaker at 165 rpm and 25°C. After 3 days of fermentation, the biomass was harvested by centrifugation (10,000 rpm, 4°C, and 20 min) and then washed thoroughly with sterile ultrapure water for three times. To prepare IPE, 10 g of biomass (wet weight) was re-suspended in sterile water and subsequently sonicated using a SONICS VCX150 ultrasonic cell disruptor for 10 min at 60% amplitude. The cell debris was removed by centrifugation, and the supernatant was diluted to 50 mL, which was donated as IPE.

### Synthesis of AuNPs

Biosynthesis of AuNPs was carried out by mixing specific volume of IPE and  $\text{HAuCl}_4$  stock solution without any other extraneous chemicals. The influences of reaction conditions including IPE addition, initial gold ion concentration, and solution pH were evaluated. To check the effect of IPE addition, 10, 20, 40, and 80 mL of IPE were respectively mixed with  $\text{HAuCl}_4$  aqueous solution, and the mixture was diluted to 100 mL with the final gold ion concentration of 1 mM. Amount of 80 mL of IPE was mixed with  $\text{HAuCl}_4$  aqueous solution with the final gold ion concentration of 0.5, 1.0, 1.5, and 2.0 mM to investigate the effect of initial gold ion concentration. As for the effect of solution pH, 80 mL of IPE was mixed with  $\text{HAuCl}_4$  aqueous solution with the final concentration of 1.0 mM, and the pH was adjusted with 0.1 M NaOH or HCl to 2.0, 4.0, 6.0, 8.0, 10.0, and 12.0. The mixtures above were incubated at 165 rpm and 30°C. The formation of AuNPs was monitored by visual inspection of the color change and measuring the UV-vis spectra of the reaction mixture.

### Characterization of AuNPs

The formation of AuNPs was further confirmed by UV-vis spectroscopic measurement of the reaction mixture solution, which was performed on a Shimadzu UV-2450 spectrophotometer (Shimadzu Corp., Kyoto, Japan) (range 400 to 700 nm) with ultrapure water as the reference, and operated at a resolution of 1 nm. X-ray diffraction (XRD) analysis of the biogenic AuNPs was done on a Bruker D8 ADVANCE X-ray diffractometer (Bruker Corp., Billerica, MA, USA) equipped with Cu  $\text{K}\alpha$  radiation ( $\lambda = 0.154$  nm), operated at a voltage of 40 kV and a current of 40 mA. The samples for XRD analysis were prepared by dropping the reaction solutions on glass substrates, followed by air drying. Analysis was made between the  $2\theta$  ranges of 20° to 90° with a step size of 0.02°. The transmission electron microscopic (TEM) study was carried out to determine the morphology and dimension of the synthesized AuNPs, which was conducted on a Hitachi-7650 instrument

(Hitachi Ltd., Tokyo, Japan) operated at an accelerating voltage of 80 kV. The samples for TEM study were prepared by dropping two or three drops of the reaction solution onto carbon-coated copper TEM grids. The extra fraction was removed using a blotting paper and then dried at room temperature. Fourier transform infrared (FTIR) spectroscopic measurement was carried out to identify the potential functional groups responsible for the reduction of gold ions and stabilization of the synthesized AuNPs, which was recorded on a PerkinElmer 1725X FTIR spectrometer. The AuNPs were collected by centrifugation (12,000 rpm, 4°C, and 20 min) and subsequently washed three times to remove free proteins or other compounds present in the reaction solution, followed by vacuum freeze-drying. The original IPE was also vacuum freeze dried and then subjected to FTIR measurement.

#### Catalytic application of AuNPs in 4-NA degradation

The degradation of 4-NA by  $\text{NaBH}_4$  was studied as a model reaction to explore the catalytic activity of bio-synthesized AuNPs. Typically, 1 mL of AuNPs solution (average size of 6.07 nm, 0.19 mg/mL) was added to a flask containing 25 mL of 0.5 mM 4-NA solution and 25 mL of 50 mM  $\text{NaBH}_4$  solution to trigger the catalytic reaction. Blank control without the addition of AuNPs was also conducted. The degradation of 4-NA was monitored by measuring the UV-vis spectra of the reaction mixture at a time interval of 3 min in the range of 250 to 500 nm. The decrease in the absorption peak centered at 380 nm with time indicated the reduction of 4-NA, and the increase in the absorption peak at about 300 to 310 nm indicated the formation of the corresponding reaction product of *p*-phenylenediamine (*p*-PDA). Different volumes of AuNPs solution were added to the above mixture to evaluate the effect of catalyst addition on the degradation process.

## Results and discussion

#### Visual inspection of AuNPs' formation

On mixing IPE with  $\text{HAuCl}_4$  aqueous solution, the color of the mixtures changed gradually from pale yellow to brown, purple, pink, or bluish violet under different reaction conditions, visually showing the formation of AuNPs. The intensity of the colors increased with time, then reached saturation, and remained unchanged even after 2 months at room temperature, indicating that the synthesized AuNPs were very stable and no aggregation phenomenon occurred. The stability of the AuNPs was likely to be due to the capping of some organic compounds such as proteins present in the IPE. It was reported that proteins can bind to metal nanoparticles through free amine groups or cysteine residues and via electrostatic attraction of negatively charged carboxyl or carbonyl groups, forming a coat covering the particles to

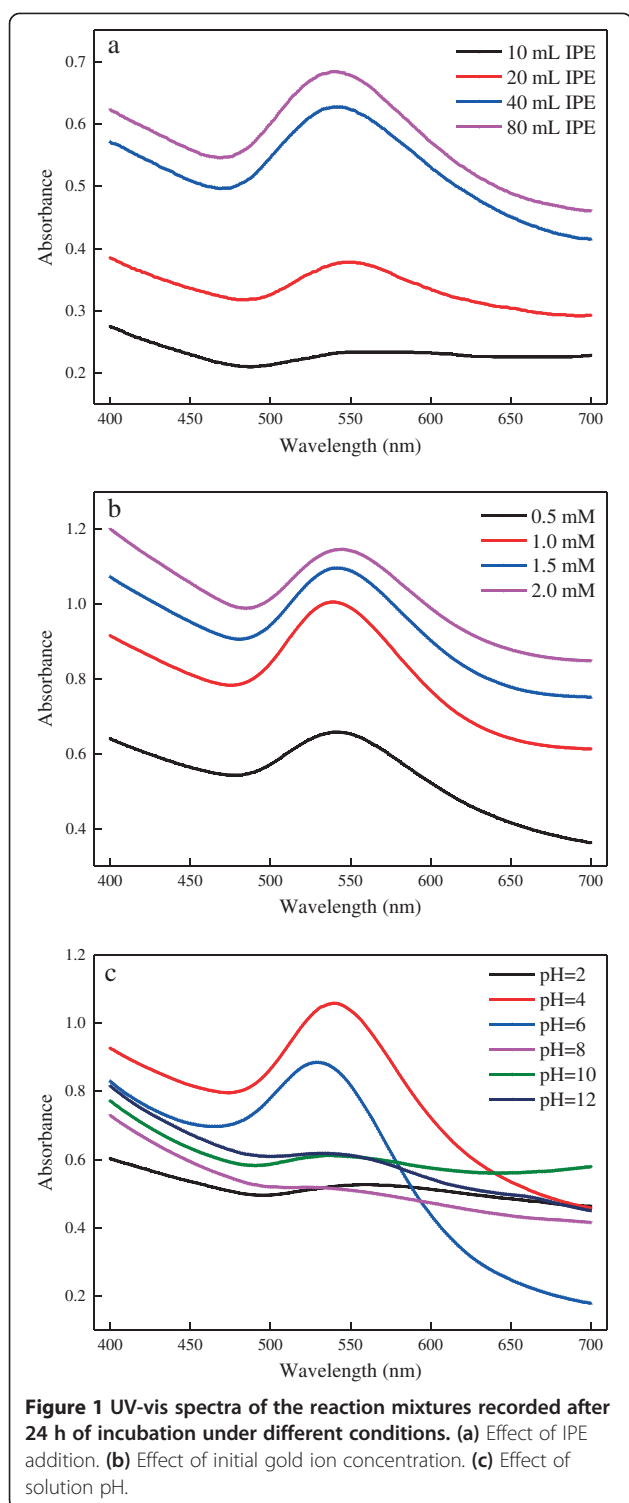
prevent agglomeration, then leading to the stabilization of AuNPs [9]. Previous researches revealed that AuNPs exhibited many vivid colors in solution, and the colors were highly dependent on the morphology and size of AuNPs [21]. The vivid colors appeared due to the excitation of surface plasmon vibrations in the AuNPs [22], which was an intrinsic property of metal nanoparticles.

#### UV-vis spectroscopy

UV-vis spectroscopy has been widely considered to be a useful technique to ascertain the formation of AuNPs [21]. Figure 1 depicted the UV-vis spectra of the reaction mixtures obtained after 24 h of incubation under various conditions. Strong absorption peaks located in the range of 520 to 560 nm were observed, further confirming the formation of AuNPs with various morphology and dimension, which was in agreement with the previous report [23]. The effect of IPE addition was shown in Figure 1a. It can be seen that the intensity of maximum absorption increased with IPE addition, indicating higher AuNPs production, since the intensity was directly proportional to the density of AuNPs [16]. In addition, a blue shift of the maximum absorption was observed as the IPE addition increased, which might be attributed to the formation of AuNPs with smaller size, further verified by TEM study. Hussein et al. [24] reported that the wavelength of maximum absorption tended to red shift as the particle size increased, which was in accordance with our results. Figure 1b illustrated the spectra of reaction mixtures with different initial gold ion concentrations. The intensity and wavelength of maximum absorption increased along with the increase of initial gold ion concentration, meaning higher production and larger particle size of AuNPs. No distinct regularity was detected with the effect of solution pH on the spectra as shown in Figure 1c, and the highest intensity was obtained with the solution pH of 4.0, while the reasons needed further research.

#### XRD analysis

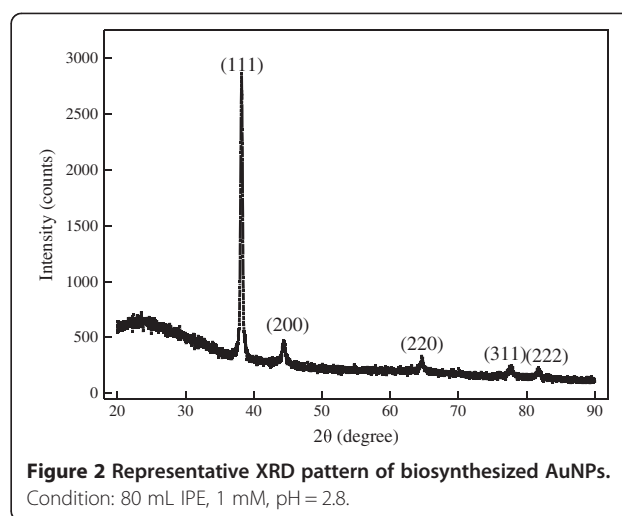
XRD analysis was performed to study the crystalline structure of the synthesized AuNPs. Figure 2 showed the representative XRD pattern, in which five diffraction peaks at about  $2\theta = 38.2, 44.6, 64.9, 77.8,$  and  $81.7$  indexed as the (111), (200), (220), (311), and (222) lattice planes of the standard face-centered cubic phase of metallic gold were observed, further indicating the formation of crystalline AuNPs. No impure peaks were detected, revealing the high purity of the formed AuNPs. The diffraction peak corresponding to the (111) phase was overwhelmingly stronger than the rest of the peaks, suggesting that (111) was the primary orientation [25]. Reaction conditions exhibited very little influences on the XRD patterns of the synthesized AuNPs, although there were slight shifts in the diffraction peak positions,



which was a common feature of the biosynthesized nanoparticles [26].

#### TEM study

The morphology and size of biosynthesized AuNPs were estimated by TEM study. Figure 3 showed the



representative TEM images of AuNPs obtained under different conditions, which illustrated the formation of AuNPs with various shapes including spherical, pseudo-spherical, triangular, truncated triangular, pentagonal, and hexagonal. The effects of IPE addition on the characteristics and particle size distributions of as synthesized AuNPs were depicted in Additional file 1: Figures S1 and S2. It can be observed that most spherical or pseudo-spherical AuNPs were relatively smaller compared with triangular, pentagonal, or hexagonal ones. With 10 mL IPE addition, many AuNPs with triangular or hexagonal shapes in the size of 100 to 500 nm were synthesized and the average size was measured to be 61.47 nm. As the IPE addition increased, the formed AuNPs exhibited narrower size distribution and smaller average particle size. When the IPE addition was increased to 80 mL, more than 90% of the AuNPs were smaller than 50 nm, almost 78% were in the range of 10 to 40 nm, and the average particle size decreased to 29.3 nm.

The impacts of initial gold ion concentration were also concerned (Additional file 1: Figures S3 and S4). When the initial concentration was 0.5 mM, AuNPs were mostly spherical or pseudo-spherical with a few triangular, more than 95% of the AuNPs were smaller than 50 nm, and the average size was 25.88 nm. As the initial concentration increased, many truncated triangular, triangular, pentagonal, or hexagonal AuNPs appeared and the average particle size increased as well. Briefly speaking, the average particle size decreased with the increase of IPE addition and increased with increasing initial gold ion concentration. It has been well accepted that gold ion was firstly reduced to form a gold atom, being a nucleus, and the latter formed gold atoms potentially aggregate to this nucleus, thus assembling a gold nanoparticle. With higher initial gold ion concentration, there was greater accessibility of the latter formed gold atoms to the nucleus, obtaining larger AuNPs [27]. Das et al. [5]

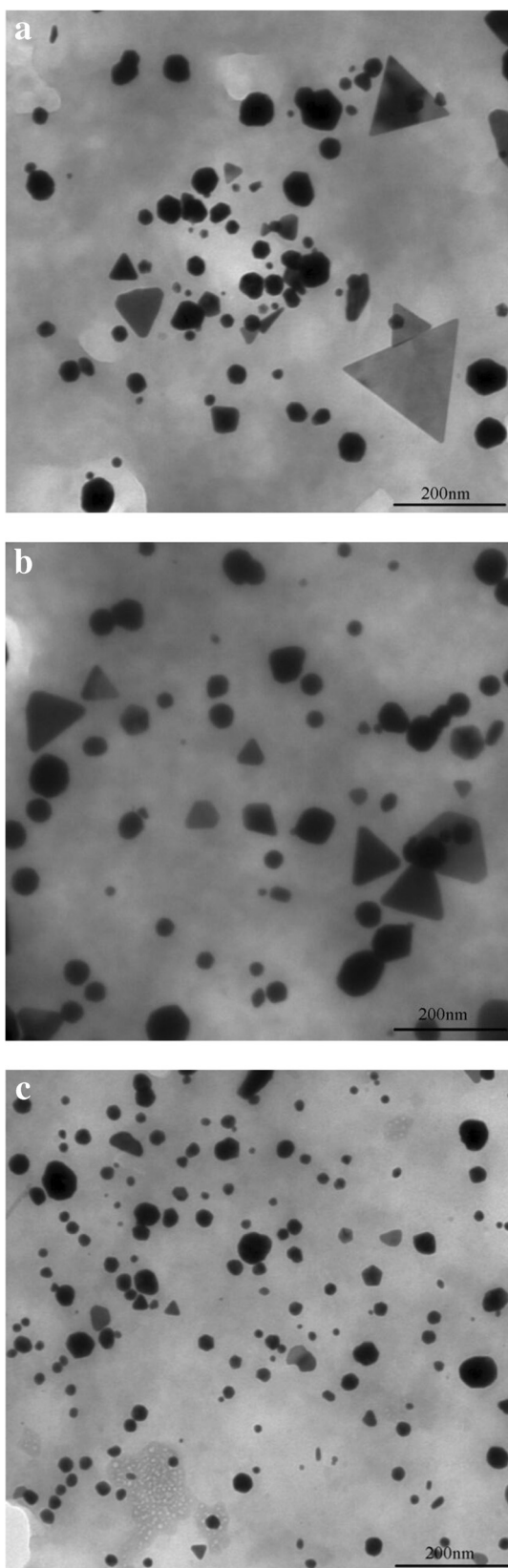


**Figure 3** Representative TEM images of AuNPs obtained under different conditions. (a) 40 mL IPE, 1.0 mM, pH = 2.7. (b) 80 mL IPE, 1.5 mM, pH = 2.5. (c) 80 mL IPE, 1.0 mM, pH = 4.0.

reported the protein-mediated synthesis of multi-shaped AuNPs, which emphasized the prominent effect of the ratio of gold ion concentration to cell-free extract, and the particle diameter increased with this ratio.

Solution pH also exhibited great influence on the characteristics and particle size distributions of the AuNPs (Additional file 1: Figures S5 and S6). With the solution pH of 2.0, AuNPs ranging from several nanometers to more than 200 nm were produced and the average particle size was measured to be 84.29 nm. As the solution changed to neutral or basic, AuNPs with much smaller and uniform size were synthesized, especially in the case of initial pH of 12.0, more than 98% of the AuNPs were smaller than 12 nm, and 90% were in 4 to 8 nm. It has been reported that reduction rate greatly affected the morphology and size of AuNPs, and slow reduction rate favored the formation of anisotropic and larger AuNPs [10]. During the synthesis of AuNPs with various solution pHs in the present research, the reaction mixture changed to bluish violet in 2 h with solution pH of 12.0. While pink color appeared after 4 h with pH of 6.0 and in the case of pH of 2.0, brown color appeared after 8 h, implying that the reaction rate increased with increasing pH, which was indirectly verified by the particle size distribution. He et al. [28] regarded solution pH as the most important parameter controlling the size and shape of AuNPs. With the solution pH of 7.0, most particles were spherical in 10 to 20 nm, and many triangular AuNPs in 50 to 400 nm were produced as the pH decreased to 4.0. Our previous research (under submission) also revealed that solution pH had noticeable impact on the location and dimension of the biosynthesized AuNPs.

#### FTIR spectroscopy measurement

FTIR spectroscopic studies were carried out to identify the possible functional groups of the biomolecules present in the IPE involved in the reduction of gold ions and stabilization of synthesized AuNPs. The original IPE showed intense and obvious absorption bands at 3,411, 2,924, 2,853, 2,109, 1,636, 1,466, 1,406, 1,055  $\text{cm}^{-1}$  (Figure 4a). The strong absorption band at 3,411  $\text{cm}^{-1}$  could be referred to the stretching vibration of O-H bond present in carbohydrates or proteins. The bands at 2,924 and 2,853  $\text{cm}^{-1}$  were due to aliphatic C-H stretching vibration of carbohydrates. The bands at 1,636 and 1,055  $\text{cm}^{-1}$  corresponded to the amide I and carbonyl stretching vibrations in the amide linkage [3]. The band at 2,109  $\text{cm}^{-1}$  could be assigned to the nitrogen compounds

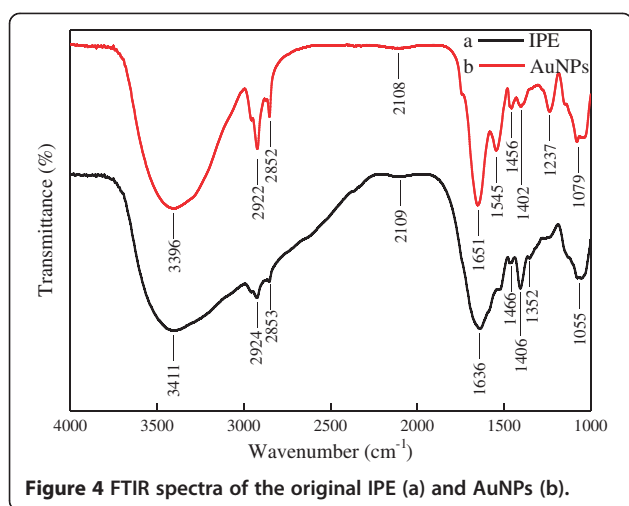


**Figure 4** FTIR spectra of the original IPE (a) and AuNPs (b).

containing triple or cumulative double bonds such as nitriles (-CN) and cyanates (-O-CN) [16]. The band at  $1,466\text{ cm}^{-1}$  might be ascribed to the methylene scissoring vibration from the proteins. The band at  $1,406\text{ cm}^{-1}$  was confirmed to the  $\text{COO}^-$  symmetric stretching vibration from the carboxyl side groups in amino acid residues of proteins [11]. Another weak band at  $1,352\text{ cm}^{-1}$  assigned to amide III was also observed. The positions of above bands were very close to those reported previously for native proteins [11].

After synthesis of AuNPs (Figure 4b), the O-H peak at  $3,411\text{ cm}^{-1}$  shifted to  $3,396\text{ cm}^{-1}$ . The amide I and carbonyl stretching peaks shifted to  $1,651$  and  $1,079\text{ cm}^{-1}$  respectively, and the band of methylene shifted to  $1,456\text{ cm}^{-1}$  as well. The weak band of amide III disappeared and two intense bands centered at  $1,545$  and  $1,237\text{ cm}^{-1}$  corresponded to amide II and C-N stretching vibrations from amines appeared. It was reported that AuNPs could interact with proteins through free amine groups or cysteine residues via electrostatic attraction of negatively charged carboxyl or carbonyl groups, forming a coat covering the particles to prevent agglomeration, thus leading to the stabilization of AuNPs [9]. Such results demonstrated that hydroxyl, amine, and carboxyl groups played important roles in the reduction process and stabilization of synthesized AuNPs. Several reports have also revealed similar conclusions. For instance, Lin et al. reported that -OH and  $-\text{NH}_2$  present on the cell surface of *Pichia pastoris* were involved in the absorption and reduction of gold ions [18]. Ogi et al. reported the participation of carbonyl group in *Shewanella algae* extract during the formation of AuNPs [29].

#### Catalytic activity of AuNPs in 4-NA degradation

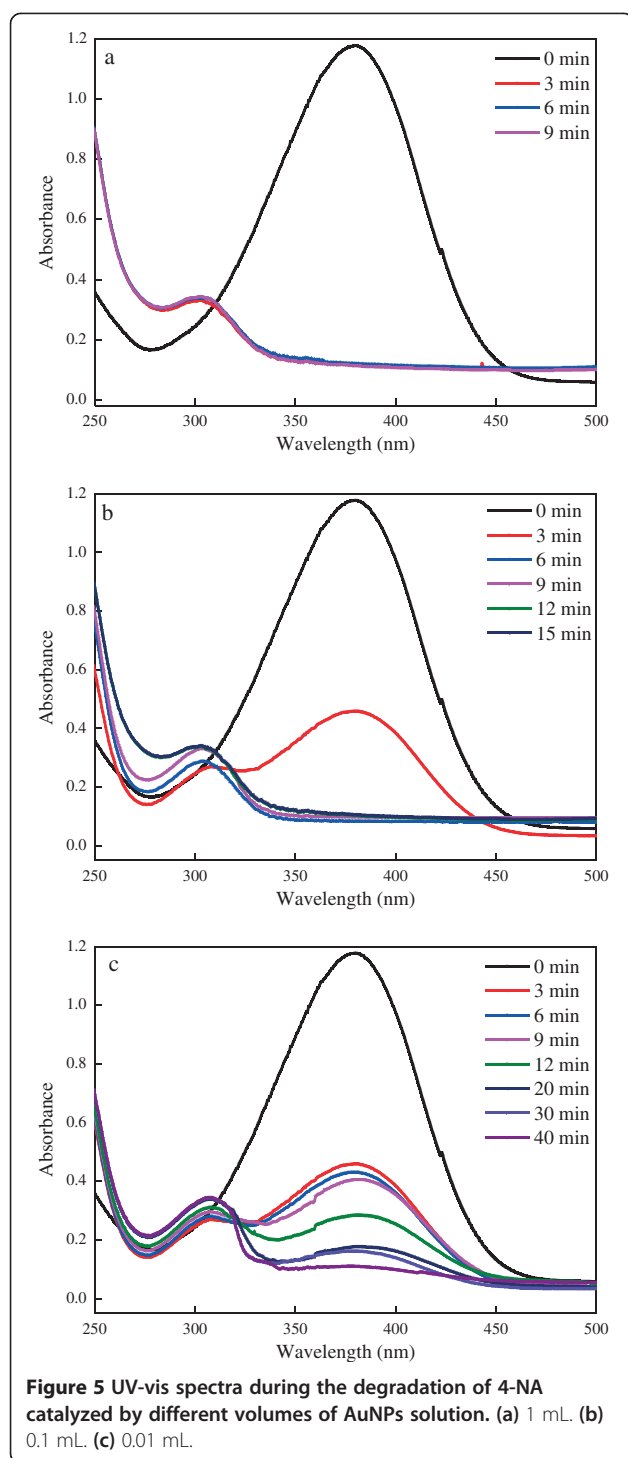
Along with the rapid development of human society, many organic contaminants have been released into the

environment. Among these contaminants, nitroaromatic compounds (NAC) are considered to be highly toxic as they exhibit serious carcinogenic and mutagenic threats to human health [30]. A promising process to eliminate NAC is to transform them into valuable amines aromatic compounds (AAC) through catalytic reduction by  $\text{NaBH}_4$  [31]. In this study, we explored the catalytic reduction of 4-NA to *p*-PDA with  $\text{NaBH}_4$  as reducing agent using biosynthesized AuNPs as catalyst. The reaction was monitored by visual inspection and using the UV-vis spectroscopy, as aqueous of 4-NA exhibited a vivid yellow color and maximum absorption at about 380 nm. Aqueous *p*-PDA was colorless and showed maximum absorption at about 300 to 310 nm [32].

Upon adding 1 mL of AuNPs solution (average size of 6.07 nm, 0.19 mg/mL) to the mixture, the color faded from yellow to colorless within 3 min. The absorption peak at 380 nm disappeared, and another absorption peak at 302 nm occurred as well (Figure 5a), indicating the rapid catalytic reduction of 4-NA. In contrast, the blank control without the addition of AuNPs showed no change in color and absorption peak even after several days, thus implying the required role of AuNPs in this reduction process, which was in accordance with many previous reports [2,11]. The effect of catalyst addition on the degradation process was also evaluated by varying the volume of AuNPs solution while keeping the other parameters constant. As shown in Figure 5, the reduction rate increased with the increasing addition of AuNPs. The time needed to completely degrade 4-NA was 3, 6, and 40 min in the cases of 1, 0.1, and 0.01 mL of AuNPs solution, respectively. Taking the reduction efficiency and catalyst addition into consideration, 0.1 mL was preferred and about 0.019 mg AuNPs (dry weight) could catalyze the complete reduction of  $12.5\text{ }\mu\text{mol}$  of 4-NA in 6 min. Since the concentration of  $\text{NaBH}_4$  much exceeded than that of 4-NA (100-fold), the kinetic reduction was considered to be pseudo-first order. The logarithm of the absorbance of 4-NA at 380 nm ( $\ln A$ ) will then decrease linearly with reaction time, and the calculated slope could be the rate constant ( $k$ ) of the reaction. In this study, the  $k$  value was calculated to be  $0.065\text{ min}^{-1}$ .

#### Conclusions

In this study, IPE of *P. sanguineus* as reducing and stabilizing agents was used to successfully synthesize AuNPs with various shapes and dimensions. The synthetic process was simple, clean, and could be an alternative to existing physical and chemical methods. Visual inspection, UV-vis spectroscopic measurement, XRD analysis, and TEM observation confirmed the formation and characteristics of AuNPs, which was highly affected by reaction conditions. FTIR analysis implied the interaction between



AuNPs and protein extract by functional groups including hydroxyl, amine, and carboxyl, which were possibly responsible for the reduction of gold ions and stabilization. The biosynthesized AuNPs could effectively catalyze the degradation of 4-NA, and 0.019 mg of AuNPs with average size of 6.07 nm was optimized to completely degrade 12.5  $\mu\text{mol}$  of 4-NA in 6 min. It was

suggested that the IPE of *P. sanguineus* could be a potential medium to synthesize AuNPs with high catalytic activity in degradation of organic contaminants.

## Additional file

**Additional file 1: Figure S1.** TEM images of AuNPs synthesized with different IPE additions. **Figure S2.** Particle size histograms of AuNPs synthesized with different IPE additions (measured more than 300 nanoparticles). **Figure S3.** TEM images of AuNPs synthesized with different initial gold ion concentrations. **Figure S4.** Particle size histograms of AuNPs synthesized with different initial gold ion concentrations (measured more than 300 nanoparticles). **Figure S5.** TEM images of AuNPs synthesized with different initial solution pHs. **Figure S6.** Particle size histograms of AuNPs synthesized with different initial solution pHs (measured more than 300 nanoparticles).

## Abbreviations

4-NA: 4-nitroaniline; AuNPs: gold nanoparticles; FTIR: Fourier transform infrared; IPE: intracellular protein extract; NaBH<sub>4</sub>: sodium borohydride; p-PDA: p-phenylenediamine; *P. sanguineus*: *Pycnoporus sanguineus*; TEM: transmission electron microscopy; XRD: X-ray diffraction.

## Competing interests

The authors declare that they have no competing interests.

## Authors' contributions

CS designed and performed the experiment, analyzed the results, and drafted the manuscript. NZ supervised the work and revised the manuscript. YC helped to analyze the results and modify the manuscript. PW performed the tests on the samples. All authors read and approved the final manuscript.

## Acknowledgements

The authors would like to thank National Natural Science Foundation of China (51178191) and Program for New Century Excellent Talents in University (NCET-11-0166) for the financial support.

Received: 10 January 2015 Accepted: 10 March 2015

Published online: 25 March 2015

## References

- Narayanan KB, Sakthivel N. Biological synthesis of metal nanoparticles by microbes. *Adv Colloid Interfac.* 2010;156:1–13.
- Srivastava SK, Yamada R, Ogino C, Kondo A. Biogenic synthesis and characterization of gold nanoparticles by *Escherichia coli* K12 and its heterogeneous catalysis in degradation of 4-nitrophenol. *Nanoscale Res Lett.* 2013;8:70.
- Suresh AK, Pelletier DA, Wang W, Broich ML, Moon JW, Gu BH, et al. Biofabrication of discrete spherical gold nanoparticles using the metal-reducing bacterium *Shewanella oneidensis*. *Acta Biomater.* 2011;7:2148–52.
- Reith F, Etschmann B, Grosse C, Moors H, Benotmane MA, Monsieus P, et al. Mechanisms of gold biomineralization in the bacterium *Cupriavidus metallidurans*. *PNAS.* 2009;106:17757–62.
- Das SK, Das AR, Guha AK. Microbial synthesis of multishaped gold nanostructures. *Small.* 2010;6:1012–21.
- Xie JP, Lee JY, Wang DIC, Ting YP. Identification of active biomolecules in the high-yield synthesis of single-crystalline gold nanoplates in algal solutions. *Small.* 2007;3:672–82.
- Annamalai A, Christina VLP, Sudha D, Kalpana M, Lakshmi PTV. Green synthesis, characterization and antimicrobial activity of Au NPs using *Euphorbia hirta* L. leaf extract. *Colloid Surface B.* 2013;108:60–5.
- Das SK, Liang JN, Schmidt M, Laffir F, Marsili E. Biomineralization mechanism of gold by zygomycete fungi *Rhizopus oryzae*. *ACS Nano.* 2011;5:6165–73.
- Binupriya AR, Sathishkumar M, Vijayaraghavan K, Yun SI. Bioreduction of trivalent aurum to nano-crystalline gold particles by active and inactive cells and cell-free extract of *Aspergillus oryzae* var. *viridis*. *J Hazard Mater.* 2010;177:539–45.

10. Xie JP, Lee JY, Wang DIC, Ting YP. High-yield synthesis of complex gold nanostructures in a fungal system. *J Phys Chem C*. 2007;111:16858–65.
11. Das SK, Dickinson C, Lafir F, Brougham DF, Marsili E. Synthesis, characterization and catalytic activity of gold nanoparticles biosynthesized with *Rhizopus oryzae* protein extract. *Green Chem*. 2012;14:1322–34.
12. Castro-Longoria E, Vilchis-Nestor AR, Avalos-Borja M. Biosynthesis of silver, gold and bimetallic nanoparticles using the filamentous fungus *Neurospora crassa*. *Colloid Surface B*. 2011;83:42–8.
13. Tripathi RM, Gupta RK, Singh P, Bhadwal AS, Shrivastav A, Kumar N, et al. Ultra-sensitive detection of mercury (II) ions in water sample using gold nanoparticles synthesized by *Trichoderma harzianum* and their mechanistic approach. *Sensor Actuat B*. 2014;204:637–46.
14. Kumar SA, Peter YA, Nadeau JL. Facile biosynthesis, separation and conjugation of gold nanoparticles to doxorubicin. *Nanotechnology*. 2008;19:495101.
15. Sawle BD, Salimath B, Deshpande R, Bedre MD, Prabhakar BK, Venkataraman A. Biosynthesis and stabilization of Au and Au–Ag alloy nanoparticles by fungus, *Fusarium semitectum*. *Sci Technol Adv Mater*. 2008;9:035012.
16. Ahmad T, Wani IA, Manzoor N, Ahmed J, Asiri AM. Biosynthesis, structural characterization and antimicrobial activity of gold and silver nanoparticles. *Colloid Surface B*. 2013;107:227–34.
17. Narayanan KB, Sakthivel N. Synthesis and characterization of nano-gold composite using *Cylindrocylindrium floridanum* and its heterogeneous catalysis in the degradation of 4-nitrophenol. *J Hazard Mater*. 2011;189:519–25.
18. Lin LQ, Wu WW, Huang JL, Sun DH, Waithera NM, Zhou Y, et al. Catalytic gold nanoparticles immobilized on yeast: from biosorption to bioreduction. *Chem Eng J*. 2013;225:857–64.
19. Fokina O, Eipper J, Winandy L, Kerzenmacher S, Fischer R. Improving the performance of a biofuel cell cathode with laccase-containing culture supernatant from *Pycnoporus sanguineus*. *Bioresour Technol*. 2015;175:445–53.
20. Sanghi R, Verma P, Puri S. Enzymatic formation of gold nanoparticles using *Phanerochaete chrysosporium*. *Adv Chem Eng Sci*. 2011;1:154–62.
21. Pimprikar PS, Joshi SS, Kumar AR, Zinjarde SS, Kulkarni SK. Influence of biomass and gold salt concentration on nanoparticle synthesis by the tropical marine yeast *Yarrowia lipolytica* NCIM 3589. *Colloid Surface B*. 2009;74:309–16.
22. Kalishwaralal K, Deepak V, Pandian SRK, Kottaisamy M, Barath Mani Kanth S, Kartikeyan B, et al. Biosynthesis of silver and gold nanoparticles using *Brevibacterium casei*. *Colloid Surface B*. 2010;77:257–62.
23. Verma VC, Singh SK, Solanki R, Prakash S. Biofabrication of anisotropic gold nanotriangles using extract of endophytic *Aspergillus clavatus* as a dual functional reductant and stabilizer. *Nanoscale Res Lett*. 2011;6:16–22.
24. Hussein MI, El-Aziz MA, Badr Y, Mahmoud MA. Biosynthesis of gold nanoparticles using *Pseudomonas aeruginosa*. *Spectrochim Acta A*. 2007;67:1003–6.
25. Aromal SA, Philip D. *Benincasa hispida* seed mediated green synthesis of gold nanoparticles and its optical nonlinearity. *Phys E*. 2012;44:1329–34.
26. Mishra A, Tripathy SK, Wahab R, Jeong SH, Hwang I, Yang YB, et al. Microbial synthesis of gold nanoparticles using the fungus *Penicillium brevicompactum* and their cytotoxic effects against mouse mayo blast cancer C<sub>2</sub>C<sub>12</sub> cells. *Appl Microbiol Biot*. 2011;92:617–30.
27. Cai F, Li J, Sun JS, Ji YL. Biosynthesis of gold nanoparticles by biosorption using *Magnetospirillum gryphiswaldense* MSR-1. *Chem Eng J*. 2011;175:70–5.
28. He SY, Guo ZR, Zhang Y, Zhang S, Wang J, Gu N. Biosynthesis of gold nanoparticles using the bacteria *Rhodospseudomonas capsulate*. *Mater Lett*. 2007;61:3984–7.
29. Ogi T, Saitoh N, Nomura T, Konishi Y. Room-temperature synthesis of gold nanoparticles and nanoplates using *Shewanella algae* cell extract. *J Nanopart Res*. 2010;12:2531–9.
30. Singh C, Goyal A, Singhal S. Nickel-doped cobalt ferrite nanoparticles: efficient catalysts for the reduction of nitroaromatic compounds and photo-oxidative degradation of toxic dyes. *Nanoscale*. 2014;6:7959–70.
31. Mandilmath TR, Gopal B. Catalytic activity of first row transition metal oxides in the conversion of p-nitrophenol to p-aminophenol. *J Mol Catal A Chem*. 2011;350:9–15.
32. Ramtenki V, Anumon VD, Badiger MV, Prasad BLV. Gold nanoparticle embedded hydrogel matrices as catalysts: better dispersibility of nanoparticles in the gel matrix upon addition of N-bromosuccinimide leading to increased catalytic efficiency. *Colloid Surface A*. 2012;414:296–301.

**Submit your manuscript to a SpringerOpen<sup>®</sup> journal and benefit from:**

- Convenient online submission
- Rigorous peer review
- Immediate publication on acceptance
- Open access: articles freely available online
- High visibility within the field
- Retaining the copyright to your article

---

Submit your next manuscript at ► [springeropen.com](http://springeropen.com)